Smart Structures and Systems, *Vol. 31*, *No. 1* (*2023*) *29-43*
https://doi.org/10.12989/sss.2023.31.1.029

Bayesian model update for damage detection of a steel plate girder bridge

Xin Zhou [1], Feng-Liang Zhang [2], Yoshinao Goi [1] and Chul-Woo Kim*[1]

[1] *Department of Civil and Earth Resources Engineering*, *Kyoto University*, *Kyoto 615-8540*, *Japan*
[2] *School of Civil and Environmental Engineering*, *Harbin Institute of Technology*, *Shenzhen 518055*, *China*

(*Received November 26*, *2021*, *Revised April 11*, *2022*, *Accepted August 28*, *2022*)

Abstract. This study investigates the possibility of damage detection of a real bridge by means of a modal parameter-based finite element (FE) model update. Field moving vehicle experiments were conducted on an actual steel plate girder bridge. In the damage experiment, cracks were applied to the bridge to simulate damage states. A fast Bayesian FFT method was employed to identify and quantify uncertainties of the modal parameters then these modal parameters were used in the Bayesian model update. Material properties and boundary conditions are taken as uncertainties and updated in the model update process. Observations showed that although some differences existed in the results obtained from different model classes, the discrepancy between modal parameters of the FE model and those experimentally obtained was reduced after the model update process, and the updated parameters in the numerical model were indeed affected by the damage. The importance of boundary conditions in the model updating process is also observed. The capability of the MCMC model update method for application to the actual bridge structure is assessed, and the limitation of FE model update in damage detection of bridges using only modal parameters is observed.

Keywords: Bayesian model update; damage detection; field vibration test; Markov chain Monte Carlo; steel plate girder bridge

1. Introduction

Many technologies utilizing sensor information have been developed to improve efficiency and accuracy in engineering decisions. Structural health monitoring (SHM) utilizing sensor information of structures also has been widely studied to provide useful information for maintenance, including damage detection, damage localization, and prediction of structural response. Indeed, damages in structures are definable as changes in material properties even including geometric properties that reduce structural performance. Therefore, damage detection can be a valuable activity that identifies structural changes in states (Pandey and Biswas 1994, Jaishi and Ren 2006).

Initially, model update was proposed to resolve the uncertainty of numerical models, but currently, it is used widely for SHM (Carden and Fanning 2004, Worden *et al*. 2007). FE models are often used to simulate behaviors of real structures for structural analysis, response prediction, and design support. Structural analysis and prediction include the simulation of displacements, internal forces, and vibration responses in several limit states, especially during earthquakes. However, because of the limited information and modeling simplification assumptions, uncertainties such as those related to material and geometric properties and load conditions invariably exist in the system (Sehgal and Kumar 2016). Model update methods purpose to calibrate uncertain model parameters by minimizing the differences between the measurement and FE analysis. The updated model is expected to predict the response of structures and evaluate current structure conditions accurately. Model update, a combination of field testing and FE models, has become a rapidly developing trend of SHM in the field of civil engineering.

Research on the model update can be categorized into two types, one is sensitivity-based (Mottershead and Friswell 1993, Mottershead *et al*. 2006, 2011, Friswell *et al*. 1997, Friswell and Mottershead 2013, Ahmadian *et al*. 1998, Jaishi and Ren 2005, Mares *et al*. 2006, Govers and Link 2010) and the other is Bayesian-based (Beck and Katafygiotis 1998, Katafygiotis and Beck 1998, Au and Beck 1999, Beck and Au 2002, Beck and Yuen 2004, Muto and Beck 2008, Goller and Schueller 2011, Goller *et al*. 2012, Yuen 2010, Lam *et al*. 2015, 2018). Sensitivity-based methods rely on the deterministic assumption, whereas Bayesian-based methods rely on the probabilistic assumption based on Bayes' theorem (Patelli *et al*. 2017). In terms of parameterization, Bayesian-based methods are more general than sensitivity-based methods. In Bayesian-based methods, the solution of uncertain parameters is a distribution. The Bayesian approach (Beck and Katafygiotis 1998, Katafygiotis and Beck 1998) aims to find a posterior probability of the model parameters. Applications of the Bayesian-based method to reliability analysis were investigated by Au and Beck (1999) and Beck and Au (2002). Beck and Yuen (2004) and Muto and Beck (2008) sought the most probable model from several model classes. Goller and Schueller (2011) and Goller *et al*. (2012) investigated uncertainties in the Bayesian model update and

*Corresponding author, Ph.D., Professor,
E-mail: kim.chulwoo.5u@kyoto-u.ac.jp

http://www.techno-press.org/?journal=sss&subpage=7
ISSN: 1738-1584 (Print), 1738-1991 (Online)

weighting factors of each mode in the objective function. Yuen (2010) and Lam *et al*. (2015, 2018) extended the applicability and efficiency of the Bayesian-based method. Xin *et al*. (2019) and Ramancha *et al*. (2020, 2022) studied the application in nonlinear systems. Jang and Smyth (2017), Song *et al*. (2018), Bassoli *et al*. (2018), Tran-Ngoc *et al*. (2020), Liu *et al*. (2021) and Zhou *et al*. (2022) investigated the model updating on actual structures.

In the Bayesian model update problem, generating samples directly from the posterior distribution is impossible because of the complexity of the posterior PDF (Lye *et al*. 2021). The Markov chain Monte Carlo (MCMC) algorithm (Tierney 1994, Mosegaard and Tarantola 1995), especially the Metropolis-Hasting (MH) algorithm (Metropolis *et al*. 1953, Hastings 1970), has been a popular sampling method for inverse problems. However, as the number of dimensions increases, the convergence of the MCMC algorithm would become excessively slow. Several advanced MH sampling methods were also developed recently to improve the convergence speed. Beck and Au (2002) introduced a sequence of intermediate distributions to converge on target distribution so-called Adaptive MH algorithm (AMH), and Ching and Chen (2007) used a similar approach in the transitional Markov chain Monte-Carlo (TMCMC) method. Goller *et al*. (2011) proposed parallelized MCMC, which can greatly accelerate the sampling procedure. The sampling method would only affect the efficiency of sampling, and there is no difference in the accuracy.

The accuracy of identified dynamic properties by system identification links directly to the accuracy of modal parameter-based model updating. Dynamic properties such as natural frequencies and mode vectors identified from vibration data are the most widely used in the model updating system because the vibration test is easy to implement (Simoen *et al*. 2015). Many methods might be used for modal identification, such as stochastic subspace identification (SSI) (Brincker and Andersen 2006, Van Overschee and De Moor 2012) and fast Bayesian FFT (Au 2011, Au *et al*. 2013, Ni and Zhang 2021). SSI is a popular approach in the time domain, whereas fast Bayesian FFT has been developed recently as a frequency domain method. These two methods were all well applied to real structures (Lam *et al*. 2015, 2018, Yin *et al*. 2012, Chaudhry *et al*. 2009, Zhang *et al*. 2021, Ni *et al*. 2022).

The FE model updated using modal parameters of the structure might provide a useful tool to analyze the present state of structures. Nevertheless, few reported studies have examined modal parameter-based model updating for actual structures, especially for bridges. The FE models of bridge structures usually are much more complex than laboratory structures, which would bring great difficulties during model updating. Moreover, the capability of model updating methods to detect structural damage in real bridges is also not well verified. There are inevitably various kinds of damage existing in actual structures, like corrosion and crack, which are significant for structural safety. Damage to structures is definable as one type of uncertainties in the system that can adversely affect system performance. Therefore, damage detection can be turned into a problem to identify changes in structural integrity between different statuses. In other words, the model update also can detect structural damage theoretically. Therefore, a full investigation of damage detection by the model update on an actual bridge is necessary.

This paper presents discussions on the feasibility of damage detection for real bridges using modal parameter-based model update. MCMC model update is investigated using data from field vibration tests conducted on an actual steel plate girder bridge. The classic MH method is taken as the sampling algorithm. The dynamic properties identified using the fast Bayesian FFT were adopted to calibrate uncertain structural parameters. Two cracks were applied on the target bridge to simulate damage of different degrees. The stiffness of steel and concrete and the spring constants were chosen as the update parameters. For the concerns of the boundary conditions, two model classes were proposed for the model update.

2. Bayesian model update by MCMC algorithm

2.1 Bayesian model update

The Bayesian model update is expected to acquire the posterior probability of uncertain parameter θ given the condition of system response D, i.e., $P(\theta|D)$. Consequently, the essence of the model updating problem is using limited information from an actual system to update model parameters in the FE model. The system response D in the modal parameter-based model update includes natural frequencies and incomplete mode vectors.

The posterior probability density function (PDF), $P(\theta|D)$, is written as shown in Eq. (1) following Bayes theorem.

$$P(\theta|D) = \frac{P(D|\theta)P(\theta)}{P(D)} \tag{1}$$

In that equation, $P(D)$ is a normalizing constant. Also, $P(\theta)$ is the prior PDF, which is assumed to follow a uniform distribution, leading it also to be a normalizing constant. The likelihood function $P(D|\theta)$ stands for the conditional probability of D given θ ($\theta \in \mathbb{R}^{N_\theta}$), where N_θ represents the number of uncertain parameters.

Because $P(\theta)/P(D)$ is a normalizing constant, the posterior PDF $P(\theta|D)$ is proportional to the likelihood function $P(D|\theta)$. Eq. (1) is then rewritten as

$$P(\theta|D) \propto P(D|\theta) \tag{2}$$

2.2 Likelihood function

In many studies (Goller *et al*. 2012, Lam *et al*. 2015, Vanik *et al*. 2000), formulations of likelihoods of several types are discussed. Let the likelihood function in Eq. (2) be written as Eq. (3).

$$P(D|\theta) = \prod_{i=1}^{N_m} P\left(\hat{f}_i|\theta\right) P(\hat{\varphi}_i|\theta) \tag{3}$$

Therein, $\hat{f}_i$ and $\hat{\varphi}_i$ denote the identified natural frequency and mode vector of the ith mode from the vibration test, respectively; N_m represents the total number of modes.

Eq. (3) includes the probability of the measured natural frequency and mode vector under a given uncertain parameter vector θ. These two components will be discussed separately.

2.2.1 Prediction error of natural frequencies

First, define the prediction-error vector of ith natural frequencies $e_{f,i}$. The absolute error $e_{f,i}$ between the measured and calculated fundamental frequencies is definable as follows.

$$e_{f,i} = \hat{f}_i - f_i(\theta), \tag{4}$$

where $f_i(\theta)$ signifies the ith natural frequency under the given uncertain parameter vector θ obtained from the FE model.

Because of the difficulty of comparing the absolute error between different modes directly, the relative error $\bar{e}_{f,i}$ shown in Eq. (5) is considered.

$$\bar{e}_{f,i} = \frac{e_{f,i}}{\hat{f}_i} = \frac{\hat{f}_i - f_i(\theta)}{\hat{f}_i} \tag{5}$$

Presume the relative error $\bar{e}_{f,i}$ follows a normal distribution with zero mean and variance $\sigma_{f,i}^2$, i.e., $\bar{e}_{f,i} \sim N(0, \sigma_{f,i}^2)$. The PDF of measured natural frequencies $\hat{f}_i$ under the parameter vector θ is defined as follows.

$$P(\hat{f}_i|\theta) = c_{f,i} e^{-\bar{e}_{f,i}^2/2\sigma_{f,i}^2} \tag{6}$$

Therein, $c_{f,i}$ stands for the normalizing constant.

2.2.2 Prediction error of mode shapes

For convenience, all mode shape vectors are normalized, i.e., $\|\varphi_i\| = \|\hat{\varphi}_i\| = 1$ ($\varphi_i \in \mathbb{R}^N, \hat{\varphi}_i \in \mathbb{R}^N$) where φ_i stands for the ith mode shape under the given uncertain parameter vector θ obtained from the FE model. Also, N denotes the number of measurement points. The identified mode shape vector $\hat{\varphi}_i$ can be decomposed as

$$\hat{\varphi}_i = \hat{\varphi}_{i\_\varphi_i} + \hat{\varphi}_{i\_\varphi_{i2}}. \tag{7}$$

Therein $\hat{\varphi}_{i\_\varphi_i} (= \langle \varphi_i, \hat{\varphi}_i \rangle \varphi_i)$ denotes the projection of the vector $\hat{\varphi}_i$ on the φ_i, in which $\langle \varphi_i, \hat{\varphi}_i \rangle$ represents the inner product of the vector φ_i and $\hat{\varphi}_i$. Let $\varphi_{i\perp}$ denotes the orthogonal complement of the vector $\hat{\varphi}_i$. $\hat{\varphi}_{i\_\varphi_{i\perp}}$, the projection of the vector $\hat{\varphi}_i$ on the $\varphi_{i\perp}$, represents the difference between the measured and identified mode shape vector $\hat{\varphi}_i \varphi_{i\perp}$. $\hat{\varphi}_{i\_\varphi_{i\perp}}$ is taken as the absolute prediction error of the mode shape. Therefore, the relative error $\bar{e}_{ms,i}$ is given as follows.

$$\bar{e}_{ms,i}^2 = \frac{\|\hat{\varphi}_{i\_\varphi_{i\perp}}\|^2}{\|\hat{\varphi}_i\|^2} = 1 - \langle \varphi_i, \hat{\varphi}_i \rangle^2 \tag{8}$$

Eq. (8) is rewritable as Eq. (9) using the modal assurance criterion (MAC) which defines the difference between two mode shape vectors as $MAC = \langle \varphi_i, \hat{\varphi}_i \rangle^2$.

$$\bar{e}_{ms,i}^2 = 1 - MAC \tag{9}$$

Similarly, assuming the normal distribution with zero mean and variance $\sigma_{ms,i}^2$ as the distribution of the $\bar{e}_{ms,i}$, i.e., $\bar{e}_{ms,i} \sim N(0, \sigma_{ms,i})$, then the PDF of the measured mode shape $\hat{\varphi}_i$ on the parameter vector θ can be expressed as Eq. (10).

$$P(\hat{\varphi}_i|\theta) = c_{ms,i} e^{-\bar{e}_{ms,i}^2/2\sigma_{ms,i}^2} \tag{10}$$

Vanik *et al*. (2000) reported that variances $\sigma_{f,i}^2$ and $\sigma_{ms,i}^2$ should be equal to the variances of the identified results. However, the prediction error consists of the measurement error from stochastic noise in the vibration test as well as the modeling error from the FE model. Generally, the modeling error effects are stronger than those of the measurement effects.

Because prediction errors of each mode are scaled, it is reasonable to assume that $\sigma_{f,i} = \sigma_f$ and $\sigma_{ms,i} = \sigma_{ms}$ for $(i = 1,2, \dots N_m)$. Moreover, to simplify the problem, the variance of each natural frequency and mode vector is assumed to be equal, as $\sigma_{ms} = \sigma_f = \sigma$ (Lam *et al*. 2015, 2018). However, in existing studies (e.g., Goller *et al*. 2012), the relative weightings were proposed to denote different contributions of the natural frequencies and mode vectors in the likelihood function. The weightings were defined as the ratio between variances of the frequencies and mode vectors as $\varepsilon = \sigma_{ms}^2/\sigma_f^2$. Then, the model class selection method (Beck and Yuen 2004, Muto and Beck 2008) was applied to select the most plausible class of models using system response data.

The likelihood function of the uncertain model parameters is rewritten as Eq. (11) by substituting Eqs. (6) and (10) into Eq. (3).

$$P(D|\theta) = c_l e^{-J(\theta)/2\sigma^2} \tag{11}$$

where $J(\theta) = \sum_{i=1}^{N} \left((1 - \langle \varphi_i, \hat{\varphi}_i \rangle^2) + \left(\frac{\hat{f}_i - f_i(\theta)}{\hat{f}_i} \right)^2 \right)$; c_l is the normalizing constant.

Consequently, according to Eqs. (1) and (2), the following posterior PDF of the uncertain model parameters is obtained

$$P(\theta|D) = c e^{-J(\theta)/2\sigma^2} \tag{12}$$

where $c = \frac{P(\theta)}{P(D)} c_l$.

The meaning of σ is the estimate of fraction error between the measured and calculated dynamic properties such as frequency and mode shape.

Although the PDF of uncertainties is known, it is also impossible to generate samples directly because of the difficulty of calculating this probability. Consequently, the Metropolis-Hastings (MH) algorithm (Beck and Au 2002; Ching and Chen 2007) was proposed for model update

procedures.

2.3 MH algorithm

MH algorithm (Metropolis *et al*. 1953, Hastings 1970) is one of the most popular MCMC solutions (Tierney 1994, Mosegaard and Tarantola 1995) in the Bayesian model update sampling problems. The MH method has a unique feature that can work where only the ratio of probability between two steps is known. This feature can solve the problem that the constant c in Eq. (12) is unknown. The central idea of MCMC is to turn the complex target distribution into a Markov chain model with a prescribed simple stationary probability distribution using the Monte Carlo method. The obtained sequence of samples would always converge to the target distribution. It is noted that the sampling method would only affect efficiency, not accuracy. The simulation of MH sampling is described as follows.

Presuming that the PDF of the target distribution is $p(\theta)$, θ_k is the kth sample, and θ_{k+1}^* is the candidate sample generated from $q(\theta_{k+1}^*|\theta_k)$, which is the PDF of the proposed distribution with given θ_k. The θ_{k+1}^* is then accepted with probability α_k given by Eq. (13).

$$\alpha_k = \alpha(x_k, x_{k+1}^*) = min\left\{1, \frac{p(\theta_{k+1}^*)q(\theta_k|\theta_{k+1}^*)}{p(\theta_k)q(\theta_{k+1}^*|\theta_k)}\right\} \quad (13)$$

Therein, α_k is a constraint to ensure that the stationary distribution of the Markov chain is the target distribution. If the candidate sample θ_{k+1}^* is accepted, then it would be set as the next sample of the Markov chain, $\theta_{k+1} = \theta_{k+1}^*$; otherwise, the present sample is to be the next one: $\theta_{k+1} = \theta_k$. Then, this process can be repeated to generate the Markov chain samples $\theta_0, \theta_1, \ldots \theta_n$.

The symmetric random-walk Metropolis (RWM) algorithm is an important special case of the MH method in which the Markov chain will jump with a symmetric proposed distribution, as $q(\theta_{k+1}^*|\theta_k) = q(\theta_k|\theta_{k+1}^*)$. It is taken to be the sampling algorithm in this study. Eq. (13) therefore simplifies to Eq. (14).

$$\alpha_k = \min\left\{1, \frac{p(\theta_{k+1}^*)}{p(\theta_k)}\right\} \quad (14)$$

When the proposed distribution $q(y|\theta)$ is taken to be a multidimensional normal distribution, it can be written as $N(\mu_\theta, \Sigma)$ with mean vector μ_θ, where θ is the uncertain parameter vector and covariance matrix $\Sigma = diag(\sigma_1^2, \sigma_2^2, \ldots, \sigma_{N_m}^2)$ where the σ_i stands for the standard deviation of each uncertain parameter.

The model update process is the process of sampling according to the target distribution. With a certain target function, the sampling algorithm can affect the update process efficiency. Consequently, the most significant factor that can affect the updated results is the target distribution. Without changing the methodology discussed in 2.2, the type of target distribution will not change.

Model update problems invariably include many uncertain parameters to update. In other words, the sampling process is always in high-dimensional spaces. The computational efficiency of the sampling process is an important issue in the Bayesian model updating. The flowchart of the MCMC model update method is presented in Fig. 1.

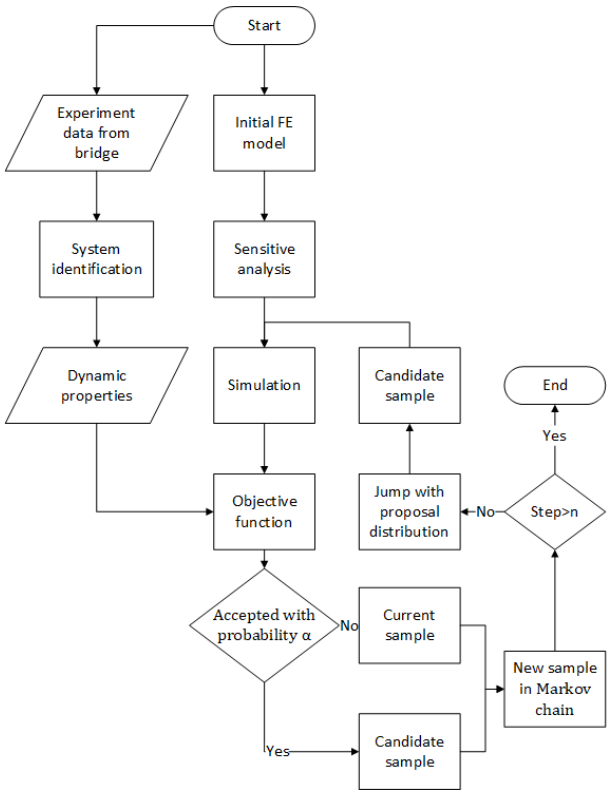

Fig. 1 Procedures of the MCMC model updating method

3. Field test and system identification

This section introduces field vibration and damage experiments conducted on an actual steel plate girder bridge. The experiment aims to investigate the modal parameters of the target bridge under different damage states.

3.1 Target bridge and finite element model

A steel plate girder bridge with concrete decks on two main girders shown in Fig. 2 is the target bridge of this study which was constructed in 1957 and was closed in 2017. The experiment was arranged before the bridge removal in 2018. The design drawings are no longer available, and most information used to establish the FE model of the bridge is from periodic inspection documents. The span length of the bridge was about 40.5 m. The bridge width was about 4 m. The bridge was supported by roller and pivot-type pin bearings.

The FE model in ABAQUS is based mainly on shell elements for the steel plate girder and concrete deck, with beam elements for the support and intermediate bracings (Fig. 3). Through eigenvalue analysis in the FE analysis, the modal properties of the model were obtained under the

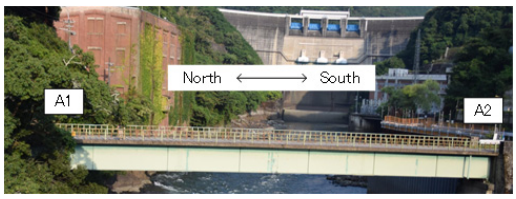

Fig. 2 Target bridge

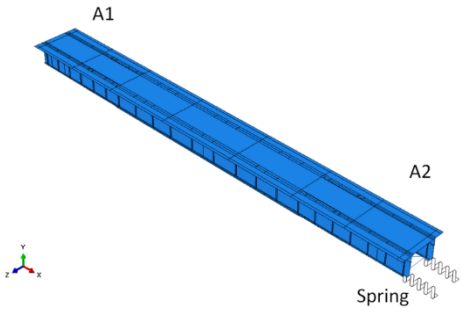

Fig. 3 FE model

specified parameters. Considering the fact that the boundary condition cannot be a perfect pin bearing in the real bridge, two springs were added to the A2 side.

3.2 Damage scenario

Artificial cracks were applied on the bridge to observe changes in structural response with different degrees of damage. Cracks propagating from the base plate bearing were selected as damage to be detected and applied to the bridge during the field experiment. Two damage scenarios were applied consecutively in this bridge, as shown in Fig. 4 and Table 1, considering safety and ease of implementation: one, called DMG1, has a cut to the lower flange at the A1 side of the upstream main girder (see also Fig. 5); the other, called DMG2, has a cut to the web plate from the cut at the lower flange, as shown in Fig. 4. The state with no artificial cracks is denoted as INT. A stopping hole is applied to prevent crack propagation from the DMG2 state.

3.3 Sensor deployment and vibration test

The vertical accelerations of the bridge were measured utilizing ten uniaxial acceleration transducers. The acceleration transducers were installed on the lower flange of two steel plate girders. Two optical sensors were set at the two ends of this bridge to record the car entrance and exit. Sensor deployment locations can be seen in Fig. 5. The experiment was conducted in three days, one day per state. During the experiments, a passenger car was used to excite the bridge. The average temperatures of these three days were 28°C, 38°C, and 43°C, respectively, during the experiment for the INT, DMG1, and DMG2 scenarios.

3.4 Material test

Concrete and steel specimens were taken from the bridge after the field experiment. The steel pieces were taken from the web plate of the main girder. The concrete cores were collected from the concrete deck. As shown in

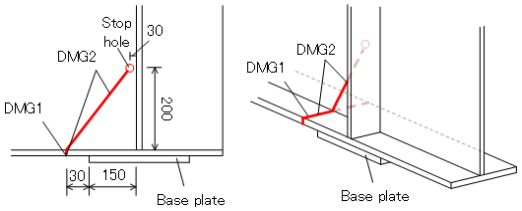

(a) Sketch of damage scenario (mm)

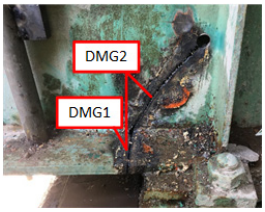

(b) Photograph of artificial cracks

Fig. 4 Artificial cracks

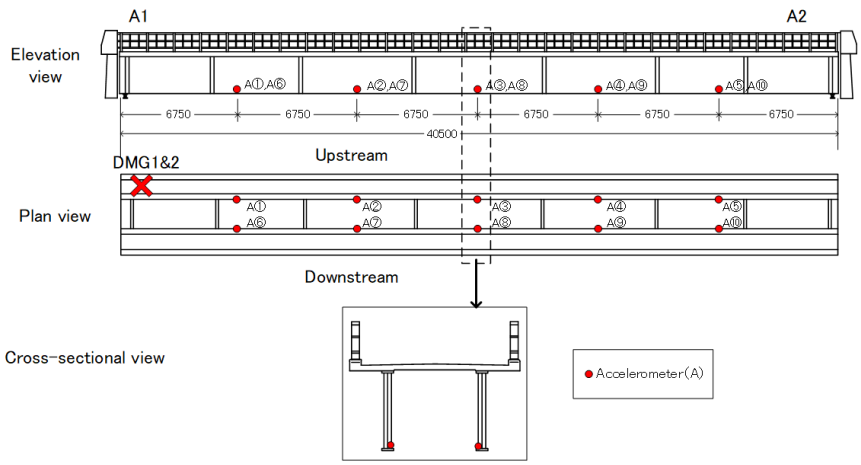

Fig. 5 Sensor deployment

Table 1 Damage scenario

Scenario	Description
INT	Intact bridge
DMG1	Cut in the lower flange at the A1 support of the upstream main girder
DMG2	Cut in the lower flange and web plate at the A1 support of the upstream main girder

Table 2 Material properties

	Max. stress (MPa)	Yield stress (MPa)	Elasticity (GPa)	Poisson's ratio
Steel	434	303	200	0.27
Concrete	46	–	28.1	0.20

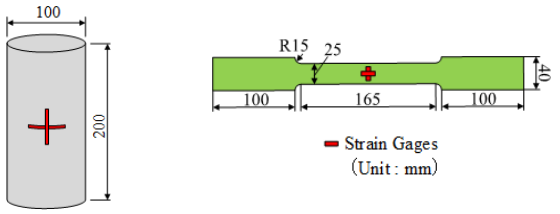

(a) Concrete (b) Steel

Fig. 6 Specimen of material test

Fig. 6, the specimen was manufactured according to JIS Z 2241 for steel and JIA A 1107 for concrete. Material properties ascertained from the material test are presented in Table 2.

3.5 Modal parameter identification

Modal parameter-based model updating aims to calibrate the modal parameters from the FE model utilizing those modal parameters identified from vibration data. Therefore, the first step is the identification of natural frequencies and mode vectors. A fast Bayesian FFT method (Au 2011, Au *et al*. 2013) was used to estimate the most probable values (MPVs) of the modal parameters as well as uncertainties in the modal parameters. Generally, when more modes are used for updating, better results are obtained. However, a non-negligible issue is that some modes cannot be identified well. If those modes are used for model updating, then it might bring some additional errors. Therefore, only the stable ones are useful in the model-updating procedure. The data length of each run was as short as 15 seconds. Therefore, the data from two runs were regarded as one group for analysis. Namely, the length would become 30 seconds.

The power spectral density (PSD) and singular value spectrum (SVS) of acceleration data measured by all ten sensors under the INT state are shown in Fig. 7. It shows six dominant peaks, which indicate well-excited modes.

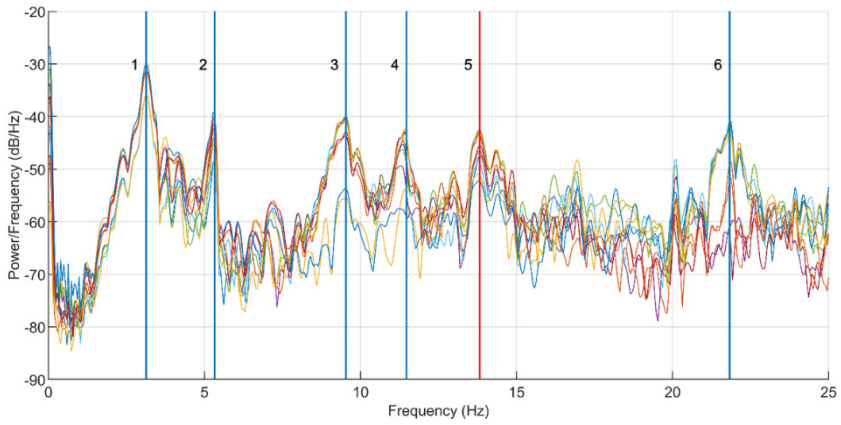

(a)

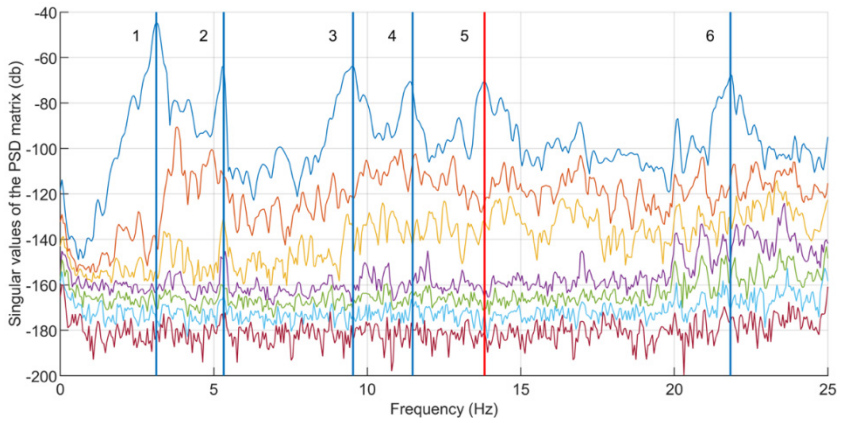

(b)

Fig. 7 (a) PSD and (b) singular value spectrum estimate for all channels

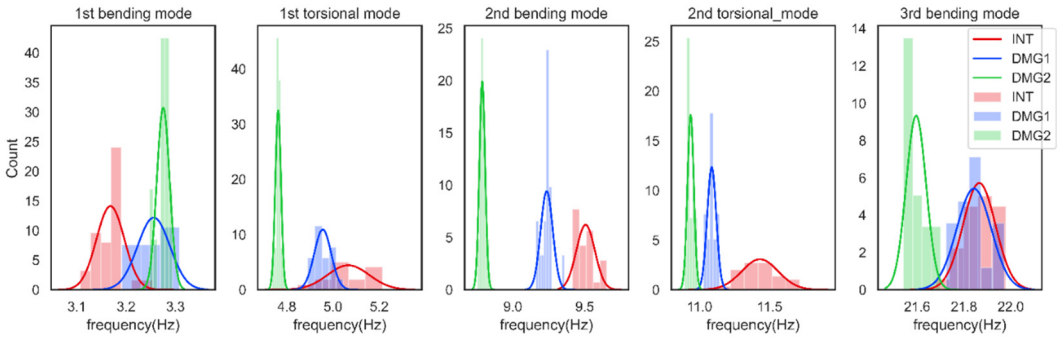

Fig. 8 Histograms with the normal distribution fit of the identified frequencies

Table 3 Identified frequencies for each damage scenario from field experiments

Mode	1st bending		1st torsional		2nd bending		2nd torsional		3rd bending	
	Freq. (Hz)	CV (%)	Freq. (Hz)	CV (%)	Freq. (Hz)	CV (%)	Freq. (Hz)	CV (%)	Freq. (Hz)	CV (%)
INT	3.17	0.91	5.07	1.81	9.51	0.69	11.43	1.16	21.86	0.32
DMG1	3.26	1.03	4.95	0.76	9.24	0.47	11.08	0.30	21.84	0.35
DMG2	3.28	0.41	4.76	0.27	8.79	0.24	10.94	0.21	21.60	0.20

*Freq. is the mean value for each mode. CV means coefficient of variation.

Table 4 MAC of the mode shapes in DMG1 and DMG2 state compared with the INT state

Mode	1st bending	1st torsional	2nd bending	2nd torsional	3rd bending
DMG1	0.9999	0.9980	0.9937	0.9156	0.9959
DMG2	0.9995	0.9920	0.9696	0.7425	0.9922

Consequently, the vibration modes of these six marked peaks were taken as the candidate modes to be updated. The natural frequencies of these six modes were close to 3 Hz, 5 Hz, 10 Hz, 11 Hz, 14 Hz, and 22 Hz, respectively. However, the mode shape of the fifth mode showed similar shapes to the third one. It was not observed in the eigenvalue analysis of the FE model. Therefore, the information of the fifth mode was not considered. For the INT state, there are 30 groups of data. Their histograms with the normal distribution fit are shown in Fig. 8 with those from damage cases (DMG1, DMG2). The MPV value and coefficient of variation (COV) of the frequency are presented in Table 3. It is noteworthy that, for the first bending mode, the natural frequency increased from INT to DMG2, whereas the trends of other modes were opposite in Table 3. One reason for the increasing frequency attributable to damage might be a change in the boundary condition at A2 abutment because of temperature changes. The longitudinal reaction at the support by deflection attributable to the dead load and temperature changes was increased. It led to an increasing spring constant at the support, which was found from sensitivity analysis for the change in stiffness and longitudinal spring constant at the support (Hirooka *et al.* 2021).

The mode shapes of INT state are presented in Fig. 9(a). It includes three bending modes from the first to the third and two torsional modes from the first to the second. Those mode shapes for the DMG1 and DMG2 states are shown respectively in Figs. 9(b) and 9(c). Table 4 presents MAC values of mode shapes between damage states (DMG1 and DMG2) and the INT state. From the MAC value in Table 4 and mode shapes in Fig. 9, we inferred the mode shape of the second torsional mode as the most damage sensitive mode, whereas other modes were nearly unchanged. Therefore, the second torsional mode might dominate the mode shape part of the model updating.

3.6 Uncertain model parameters

There are various sources of errors in modeling, e.g., simplification of the actual structure and unavailable material properties (Beck and Au 2002, Goller and Schueller 2011, Lam *et al.* 2015). Simplification refers to unmodeled or incompletely modeled in line with actual structural features, especially boundary conditions, connections, and damage. For example, actual structures have few perfect pins or other joints whereas they are usually used in the FE model. Material uncertainties often refer to the density and Young's modulus of materials. Because of corrosion or other factors, material properties usually differ from design values. Generally, it is not easy to obtain test pieces from in-service bridges because this action might cause new structural damage and block traffic.

Various damage, like corrosion and crack, inevitably exists in actual structures and affects the geometric and material properties of the system. Therefore, the modeling error problem of damaged structures would be particularly serious. Moreover, other factors such as temperature and wind would also have a similar effect. However, since the limitation of data, it is impractical to identify and model the effect of each factor. Therefore, this study only aims to identify the changes in the structure. No matter structural damage or other factors is assumed to be reflected by

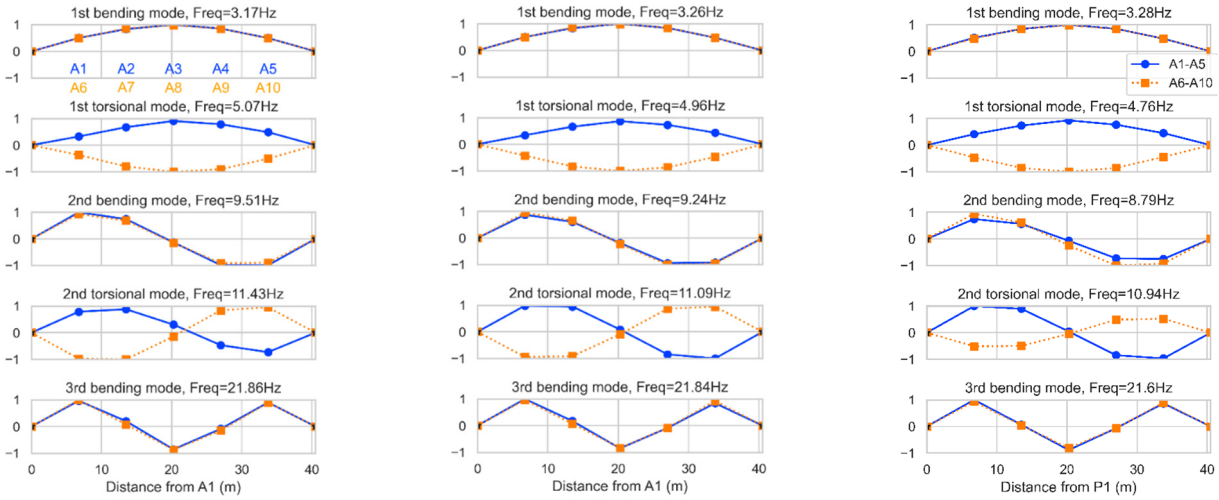

(a) INT (b) DMG1 (c) DMG2

Fig. 9 Identified mode shape

Table 5 Nominal values of parameters

Updating list	S.Elastic	RC.Elastic	Spring	S.Density	RC.Density
Nominal value	210 GPa	22.02 Gpa	5×10^4 kN/m	7850 kg/m^3	2400 kg/m^3

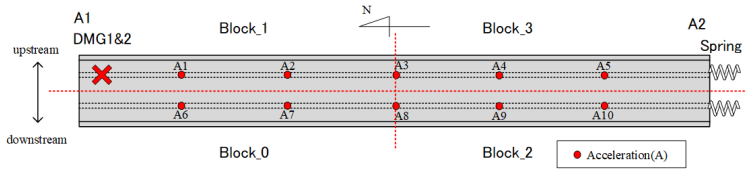

Fig. 10 Bridge blocks to be updated

uncertain model parameters for model updating. Presumably, structural damage such as cracks can also be simulated through decreased stiffness in the same part. Therefore, this assumption would be applied to the artificial cracks in the model updating process.

Five model parameters of the bridge consisting of four material parameters and one geometric parameter were selected as candidates for model updating. The candidates of material parameters include Young's modulus of steel (S.Elastic), Young's modulus of concrete (RC.Elastic), steel density (S.Density), and concrete density (RC.Density). Although material properties were obtained from material testing, they are still assumed to be unknown to simulate actual engineering situations. The candidate geometric parameters include two springs, as shown in Fig. 3. The nominal values of these parameters are shown in Table 5. Most damages occurred in bridge structures are crack and corrosion, which mainly affect the stiffness of materials and rarely change the density. Moreover, considering the fact that the experiments were conducted in a short period, the applied artificial damage introduced no loss in mass. Therefore, to simplify the problem, only the elastic modulus of steel and concrete and two spring constants were taken into account, while the density was not.

4. FE model update of the steel plate girder bridge

This section investigated the feasibility of modal parameter-based model updating of the target bridge. Model parameters of three types, such as the added spring at the A2 support and the steel and concrete stiffness, are considered in the model update. The boundary condition at the A1 support was set fixed as severe deterioration was observed. The range of steel stiffness was set as [0 GPa, 400 GPa]. The concrete stiffness range was set as [0 GPa, 40 GPa]. The range of spring constant was set as [0 kN/m, 2×10^5 kN/m]. Initial values of these parameters were set as 210 GPa for steel stiffness, 20.202 GPa for concrete stiffness, and 5×10^4 kN/m for the spring constant.

Considering the potential difference in the material properties of the different parts of the bridge, as an initial trial, a block model was proposed. In the block model, the bridge is divided into four blocks (named Block_0, Block_1, Block_2, and Block_3) to be updated as shown in Fig. 10. The model parameters include steel stiffnesses of four kinds (denoted as S.Elastic_0, S.Elastic_1, S.Elastic_2, and S.Elastic_3) corresponding to each block, with one type of spring constant (denoted as Spring), and one type of concrete stiffness (denoted as RC.Elastic).

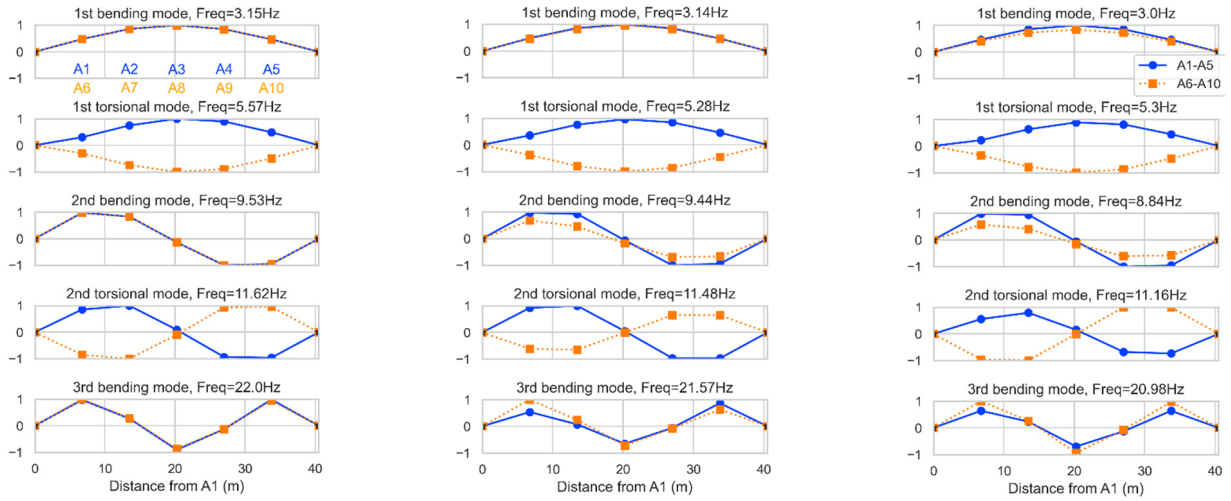

(a) Mode shape of FE model without damage

(b) Mode shape of FE model with crack for DMG2

(c) Mode shape of FE model with decreased stiffness for DMG2

Fig. 11 Analytical mode shape of FE model with different damage models

The candidate parameters will be updated in the INT state at first. The concrete deck stiffness was set as a constant in the model update for DMG1 and DMG2 states because the deck was unchanged during the experiment. Moreover, to investigate the influence of boundary conditions on the model update for damage scenarios, both schemes with and without consideration of springs as model parameters were examined.

4.1 Modeling crack in FE model

To verify whether the cracks can be simulated by the decrease of Young's modulus of the structural members, the following two cases are examined using eigenvalue analysis: a model with the crack that is the same as DMG2 and a model with decreased stiffness in Block_1 (S.Elastic_1). Fig. 11 shows mode shapes obtained from eigenvalue analysis using FE models with different damage models. For comparison with experimental mode shapes shown in Fig. 9, the analytical mode shapes presented in Fig. 11 are also taken from the same sensor location during the experiment.

The mode shapes of first bending and torsional modes might not be sensitive to damage, like those from the experiment. For the second bending mode, comparing the relative amplitude of the mode shape of the damaged (especially sensors A1 and A2 of Block_1 in Fig. 10) and undamaged (especially sensors A6 and A7 of Block_0 in Fig. 10) blocks, it can be observed that the relative amplitude of the damaged block was increased compared to the undamaged block. A similar tendency was observed in both crack-introduced and stiffness-reduced models.

For the third bending mode, comparing the relative amplitude of the mode shape of the damaged (especially the sensor A1 of Block_1) and undamaged (especially the sensor A6 of Block_0) blocks, it can be observed that the relative amplitude of the mode shape at the damaged block was decreased compared to the undamaged block. For the mode shape of the crack-introduced model, the relative amplitude of the mode shape at sensor A5 was increased compared to the amplitude of the mode shape at sensor A10. For the mode shape of the stiffness-reduced model, however, the relative amplitude of the mode shape at sensor A5 was decreased compared to the amplitude of the mode shape at sensor A10.

For the second torsional mode, the relative amplitudes of the mode shape at the damaged block of the crack-induced model were increased, whereas at the damaged block of the stiffness-reduced model were decreased. Considering that the second torsional mode was the most sensitive mode for damage, as discussed in the modal parameters identified from the experiment, using the stiffness-reduced model in the modal parameter-based model updating for damage detection could misinterpret an undamaged block as a damaged block.

4.2 FE Model updating for the initial model

All six candidate parameters in the INT state were updated first. The marginal distributions of those updated parameters are presented in Fig. 12. The identified distributions of parameters are presented by the marginal distribution because the solution space is high-dimensional. Kernel density estimation (KDE) proposed by Rosenblatt (1956) and Parzen (1962) is used to estimate the PDFs of the marginal distributions from the obtained sequence of samples. KDE can improve prediction accuracy, especially in estimating the marginal densities of the samples.

Each parameter converged to the MPV (a single peak in the PDF) is presented in Table 6. Table 7 presents the error between the simulation based on MPV in Table 6 and the experiment. The discrepancy between the simulation and experiment was reduced, in general, after model updating. For the natural frequency, except for the first bending mode, the errors of other modes are decreased. For the mode shape, the MAC value of the second torsional mode was improved from 0.9188 to 0.9657. Those updated parameters presented in Table 6 and Fig. 12 are used as reference

Table 6 Updated parameters of each bridge block under the INT state

	S.Elastic_0	S.Elastic_1	S.Elastic_2	S.Elastic_3	RC.Elastic	Spring
INT	237 GPa	131 GPa	184 GPa	180 GPa	20.8 GPa	2.86×10^4 kN/m

Table 7 Updated natural frequencies and mode shapes of the bridge under the INT state

	Mode	Measured	Before updating			Updated		
		Freq. (Hz)	Freq. (Hz)	Error (%)	MAC	Freq. (Hz)	Error (%)	MAC
INT	1st bending	3.17	3.30	4.06	0.9994	3.00	5.26	0.9958
	1st torsional	5.07	5.83	15.07	0.9981	5.48	8.14	0.9957
	2nd bending	9.51	10.16	6.84	0.9972	9.45	0.57	0.9966
	2nd torsional	11.43	12.11	5.97	0.9188	11.59	1.38	0.9657
	3rd bending	21.86	23.34	6.74	0.9926	21.91	0.20	0.9896

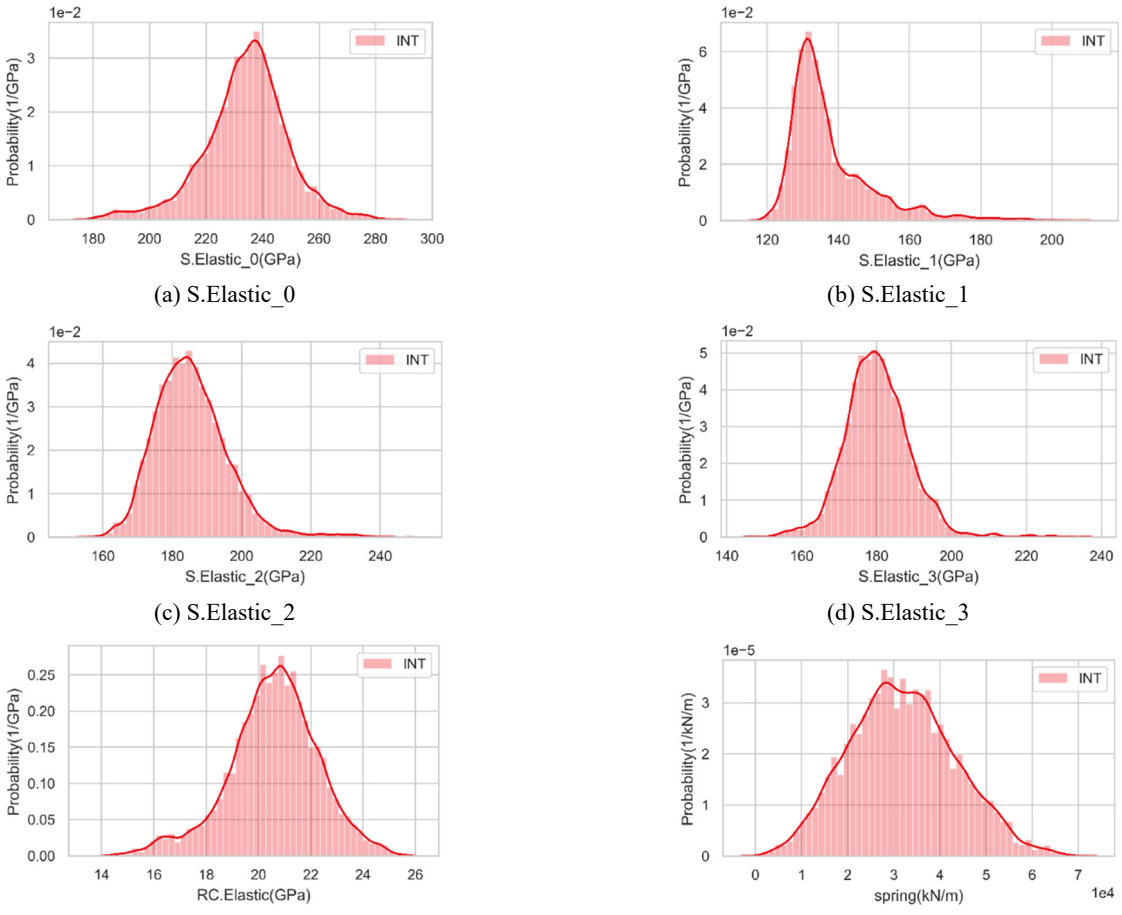

(a) S.Elastic_0 (b) S.Elastic_1

(c) S.Elastic_2 (d) S.Elastic_3

(e) RC.Elastic (f) Spring

Fig. 12 KDE of model parameters for each bridge block under the INT state.

information for damage detection using the modal parameter-based model update in section 4.3.

4.3 FE Model updating for damage detection

Model updating is conducted with acceleration data from the damaged bridge, i.e., the bridge under DMG1 and DMG2 states. For model updating of the target bridge, two updating schemes are considered. One is to set the concrete deck stiffness as a constant value in the initial model (Case 1); another is to set both the stiffness of the concrete deck and springs at the A2 support as constant values in the initial model (Case 2). The stiffness of the concrete deck and spring constant at the A2 support were set as 20.8 GPa and 2.86×10^7 N/m respectively, which are obtained from the model updating results of the INT state shown in Table 6.

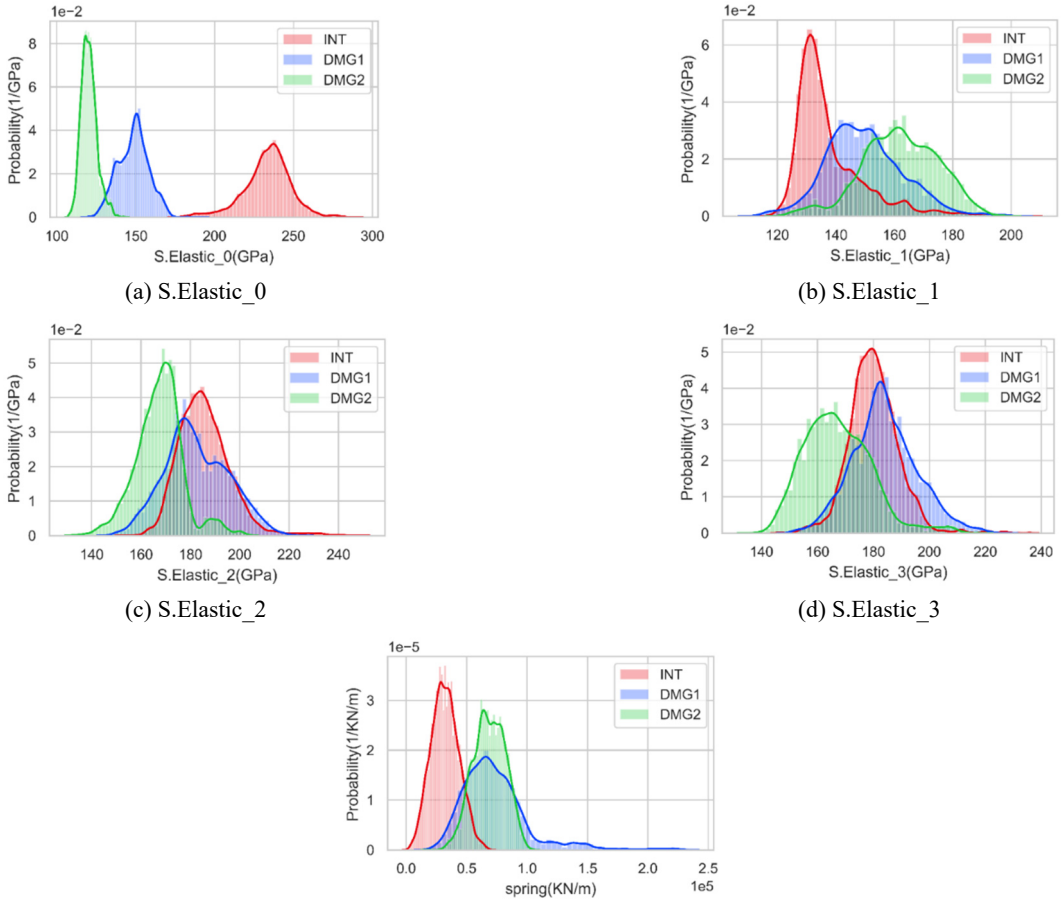

(a) S.Elastic_0 (b) S.Elastic_1

(c) S.Elastic_2 (d) S.Elastic_3

(e) Spring

Fig. 13 KDE of model parameters for the bridge block to be updated under each damage scenario (Case 1)

Table 8 Updated parameters of each bridge block under each damage scenario, DMG1 and DMG2 (Case 1)

	S.Elastic_0	S.Elastic_1	S.Elastic_2	S.Elastic_3	Spring
INT*	237 GPa	131 GPa	184 GPa	180 GPa	2.86×10^4 kN/m
DMG1 (DMG1/INT)	151 GPa (0.64)	143 GPa (1.09)	178 GPa (0.97)	182 GPa (1.01)	6.58×10^4 kN/m (2.30)
DMG2 (DMG2/INT)	118 GPa (0.50)	161 GPa (1.23)	170 GPa (0.92)	165 GPa (0.92)	6.39×10^4 kN/m (2.23)

*Values of INT are the same as those in Table 6 and are reposted for comparison.

4.3.1 Case 1: Damage detection under the scheme of setting the stiffness of the concrete deck as constant

Fig. 13 portrays the marginal distributions of updated parameters in Case 1. The MPVs of the respective parameters are presented in Table 8. Updated modal parameters using MPVs in Table 8 are presented in Table 9. The change in stiffness of Block_0 (S.Elastic_0) was observed as the most readily apparent: the MPV drops from 237 GPa in INT to 118 GPa in DMG2, as shown in Fig. 13(a), despite the application of damage to the lower flange and web of Block_1.

The Block_1 stiffness (S.Elastic_1) was increased. Comparison of stiffness changes of Block_0 (S.Elastic_0) and Block_1 (S.Elastic_1) shows that tendencies of stiffness changes in Block_2 (S.Elastic_2) and Block_3 (S.Elastic_3) are almost identical. They also show a similar distribution in the INT and DMG1 states. Only when the damage accumulated to a certain degree, the DMG2 state did a marked change occur.

The spring constant seems to change quite a lot from INT to DMG1. DMG1 and DMG2 nearly share the same distribution, as shown in Fig. 13(e). When the damage was applied to the bridge, the spring constant representing the boundary conditions changed. Because the spring strongly influences the first bending mode of simply supported girder bridges, the increase of spring constant engenders an increase in the first bending frequency: for the updated first

Table 9 Updated natural frequencies and mode shapes of the bridge under each damage scenario (Case 1)

Mode		Measured	Initial model			Updated		
		Freq. (Hz)	Freq. (Hz)	Error (%)	MAC	Freq. (Hz)	Error (%)	MAC
DMG1	1st bending	3.26	3.27	0.31	0.9997	3.11	4.60	0.9991
	1st torsional	4.96	5.81	17.14	0.9938	5.37	8.27	0.9963
	2nd bending	9.24	10.11	9.42	0.9926	9.03	2.27	0.9942
	2nd torsional	11.09	12.07	8.84	0.9900	11.27	1.62	0.9867
	3rd bending	21.84	23.19	6.18	0.9863	20.97	3.98	0.9965
DMG2	1st bending	3.28	3.27	0.30	0.9997	3.04	7.32	0.9967
	1st torsional	4.76	5.81	22.06	0.9858	5.25	10.29	0.9861
	2nd bending	8.79	10.11	15.02	0.9756	8.78	0.11	0.9890
	2nd torsional	10.94	12.07	10.33	0.9135	11.06	1.10	0.9458
	3rd bending	21.60	23.19	7.36	0.9802	20.49	5.14	0.9848

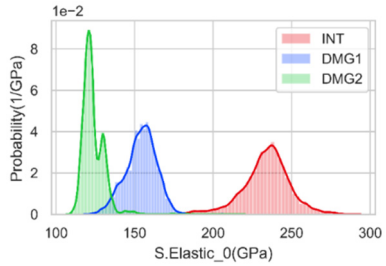

(a) S.Elastic_0

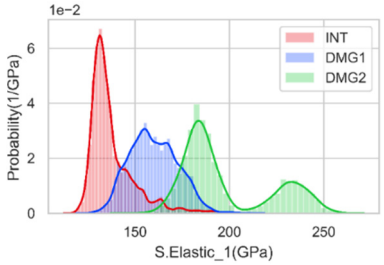

(b) S.Elastic_1

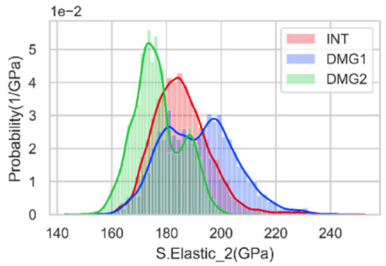

(c) S.Elastic_2

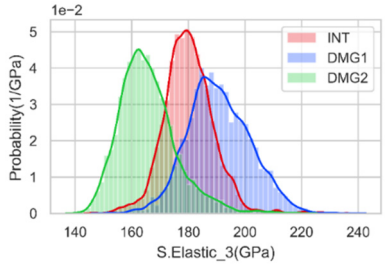

(d) S.Elastic_3

Fig. 14 KDE of model parameters for each bridge block to be updated under different damage scenarios (Case 2)

bending frequency, it changed from the 3.00 Hz as shown in Table 7 to the 3.11 Hz as shown in Table 9.

4.3.2 Case 2: Damage detection under the scheme of setting constant concrete deck and spring stiffness at the support

Fig. 14 portrays the marginal distributions of updated parameters under the update scheme of setting the stiffness of the concrete deck and springs at support A2 as constant using those values updated in INT state in Table 6. The MPVs of the respective parameters are presented in Table 10. The updated modal parameters using MPVs in Table 10 are presented in Table 11. The change in stiffness of Block_0 (S.Elastic_0) was observed as the most readily apparent. The MPV drops from 237 GPa in INT to 121 GPa in DMG2, as shown in Fig. 14(a), despite the application of damage to the lower flange and web of Block_1.

Table 10 Updated parameters for each bridge block under each damage scenario (Case 2)

	S.Elastic_0	S.Elastic_1	S.Elastic_2	S.Elastic_3
INT*	237 GPa	131 GPa	184 GPa	180 GPa
DMG1 (DMG1/INT)	157 GPa (0.66)	155 GPa (1.18)	181 GPa (0.98)	185 GPa (1.03)
DMG2 (DMG2/INT)	121 GPa (0.51)	184 GPa (1.41)	173 GPa (0.94)	162 GPa (0.90)

*Values of INT are the same as those in Table 6 and are reposted for comparison

Similarly, with the results of Case 1 in section 4.3.1 (scheme of setting the stiffness of the concrete deck as constant), the stiffness of Block_1 (S.Elastic_1) was increased. The tendencies of stiffness changes in Block_2

Table 11 Updated natural frequencies and mode shapes of the bridge under each damage scenario (Case 2)

	Mode	Measured	Initial model			Updated		
		Freq. (Hz)	Freq. (Hz)	Error (%)	MAC	Freq. (Hz)	Error (%)	MAC
DMG1	1st bending	3.26	3.16	3.07	0.9997	2.95	9.51	0.9994
	1st torsional	4.96	5.78	16.53	0.9940	5.39	8.67	0.9957
	2nd bending	9.24	10.09	9.20	0.9952	9.14	1.08	0.9958
	2nd torsional	11.08	12.06	8.75	0.9906	11.37	2.52	0.9888
	3rd bending	21.84	23.19	6.18	0.9834	21.31	2.43	0.9954
DMG2	1st bending	3.27	3.16	3.66	0.9998	2.88	12.20	0.9982
	1st torsional	4.76	5.78	21.43	0.9854	5.28	10.92	0.9848
	2nd bending	8.78	10.09	14.79	0.9767	8.93	1.59	0.9897
	2nd torsional	10.93	12.06	10.24	0.9134	11.17	2.10	0.9524
	3rd bending	21.89	23.19	7.36	0.9804	20.83	3.56	0.9814

(S.Elastic_2) and Block_3 (S.Elastic_3) fluctuated within the same range of values. In Fig. 14(c), the PDF curve of S.Elastic_2 in DMG1 state exhibits two peaks. It is noteworthy that the updated first bending frequency of DMG1 was decreased differently from Case 1 and experimentally obtained results. It underscores the importance of modeling the spring constant at the support.

4.3.3 Discussion

After updating, the difference between the simulation and experiment was decreased, as presented in Tables 7, 9, and 11. Indeed, except for the frequencies of the first bending mode, other frequencies and mode shapes were improved in all states. In the results, changes in the model parameters were observed with the applied artificial cracks. In both updating schemes described in 4.3.1 and 4.3.2, the steel stiffness shows a similar change trend. S.Elastic_0 and S.Elastic_1 changed obviously due to damage. The ratio of DMG2/INT is smaller than DMG1/INT, which indicates that the damage extent of DMG2 state is more than that of DMG1. The values of model parameters are indeed affected by changes in modal parameters due to the damage, which can be used for damage detection.

The identified damage location cannot fully fit the real damages. When the artificial damage was applied to the lower flange and web of Block_1, a decrease of S.Elastic_1 was expected. However, in both 4.3.1 and 4.3.2, the value of S.Elastic_1 increased, and the decreased one was S.Elastic_0 of Block_0. One reason for this phenomenon is using changes in stiffness to simulate cracks. As discussed in 4.1, how to model the damage in FE analysis resulted in different responses in the mode shape of the second torsional mode.

The difference between these two schemes, Case 1 in 4.3.1 and Case 2 in 4.3.2, is whether the spring is set as a constant value, or not. A comparison of the updated frequencies in Table 9 with Table 11 shows that the discrepancy between the FE model and experimental data in Table 9 is less than that in Table 11. The results indicate that the updated model, which considers the change in the spring constant, is closer to the real bridge. It also demonstrated the necessity of considering the change of boundary conditions in model updating. From this perspective, updating the boundary conditions is also a necessary choice.

5. Conclusions

This study investigates the possibility of damage detection of real bridges by means of modal parameter-based FE model updating. Vibration and damage experiments were conducted on an actual steel plate girder bridge. A fast Bayesian FFT was adopted to identify modal parameters of the bridge, such as modal frequencies and vectors, and the MH algorithm was employed to estimate the posterior distribution obtained from the Bayesian model updating method. The structural damages were simulated by decreasing material stiffness. Two model classes were proposed for model updating. Application of modal parameter-based model updating in a real bridge is then conducted using these two model classes.

The FE model was well updated by means of the modal parameter-based Bayesian model updating approach so as to match with the measured modal parameters of the actual bridge. However, it does not guarantee that the updated model parameters are meaningful even though updated modal parameters are well comparable with the measured ones. In other words, it is clear that the FE model updating has limitations in damage detection of bridges using only modal parameters, because only a limited amount of sensor information is available while the degrees of freedom of the FE model of the bridge are huge. It was observed that how the damage is modeled in FE analysis also affects the possibility of damage detection using FE model updating.

The possibility and limitations of the modal parameter-based model updating for real bridges are verified. Taking the FE model as a block model for updating can reduce the computation burden and provide information about the potential damage zone in the bridge.

Acknowledgments

This study was partly supported by a Japanese Society for the Promotion of Science (JSPS) Grant-in-Aid for Scientific Research (B) under project No. 19H02225 and National Natural Science Foundation of China under project No. 52278298. The financial supports are gratefully acknowledged.

References

Ahmadian, H., Mottershead, J.E. and Friswell, M.I. (1998), "Regularisation methods for finite element model updating", *Mech. Syst. Signal Process.*, **12**(1), 47-64. https://doi.org/10.1006/mssp.1996.0133

Au, S.K. (2011), "Fast Bayesian FFT method for ambient modal identification with separated modes", *J. Eng. Mech.*, **137**(3), 214-226. https://doi.org/10.1061/(ASCE)EM.1943-7889.0000213

Au, S.K. and Beck, J.L. (1999), "A new adaptive importance sampling scheme for reliability calculations", *Struct. Safety*, **21**(2), 135-158. https://doi.org/10.1016/S0167-4730(99)00014-4

Au, S.K., Zhang, F.L. and Ni, Y.C. (2013), "Bayesian operational modal analysis: theory, computation, practice", *Comput. Struct*, **126**, 3-14. https://doi.org/10.1016/j.compstruc.2012.12.015

Bassoli, E., Vincenzi, L., D'Altri, A.M., de Miranda, S., Forghieri, M. and Castellazzi, G. (2018), "Ambient vibration-based finite element model updating of an earthquake-damaged masonry tower", *Struct. Control Health Monitor.*, **25**(5), e2150. https://doi.org/10.1002/stc.2150

Beck, J.L. and Au, S.K. (2002), "Bayesian updating of structural models and reliability using Markov chain Monte Carlo simulation", *J. Eng. Mech.*, **128**(4), 380-391. https://doi.org/10.1061/(ASCE)0733-9399(2002)128:4(380)

Beck, J.L. and Katafygiotis, L.S. (1998), "Updating models and their uncertainties. i: Bayesian statistical framework", *J. Eng. Mech.*, **124**(4), 455-461. https://doi.org/10.1061/(ASCE)0733-9399(1998)124:4(455)

Beck, J.L. and Yuen, K.V. (2004), "Model selection using response measurements: Bayesian probabilistic approach", *J. Eng. Mech.*, **130**(2), 192-203. https://doi.org/10.1061/(ASCE)0733-9399(2004)130:2(192)

Brincker, R. and Andersen, P. (2006), "Understanding stochastic subspace identification", *Proceedings of the 24th IMAC*, St. Louis, Missouri, USA, January.

Carden, E.P. and Fanning, P. (2004), "Vibration based condition monitoring: a review", *Struct. Health Monitor.*, **3**(4), 355-377. https://doi.org/10.1177/1475921704047500

Chaudhry, R., Ravichandran, A., Hager, G. and Vidal, R. (2009), "Histograms of oriented optical flow and Binet-Cauchy kernels on nonlinear dynamical systems for the recognition of human actions", *2009 IEEE Conference on Computer Vision and Pattern Recognition*, Miami, FL, USA, June.

Ching, J. and Chen, Y.C. (2007), "Transitional Markov chain Monte Carlo method for Bayesian model updating, model class selection, and model averaging", *J. Eng. Mech.*, **133**(7), 816-832. https://doi.org/10.1061/(ASCE)0733-9399(2007)133:7(816)

Friswell, M.I. and Mottershead, J.E. (2013), *Finite Element Model Updating in Structural Dynamics*, (Vol. 38), Springer Science & Business Media.

Friswell, M.I., Mottershead, J.E. and Ahmadian, H. (1997). "Combining subset selection and parameter constraints in model updating", *Proceedings of the ASME 1997 Design Engineering Technical Conferences*, *Volume 1B*: *16th Biennial Conference on Mechanical Vibration and Noise*, Sacramento, CA, USA, September.

Goller, B. and Schueller, G.I. (2011), "Investigation of model uncertainties in Bayesian structural model updating", *J. Sound Vib.*, **330**(25), 6122-6136. https://doi.org/10.1016/j.jsv.2011.07.036

Goller, B., Broggi, M., Calvi, A. and Schueller, G. (2011), "A stochastic model updating technique for complex aerospace structures", *Finite Elem. Anal. Des.*, **47**(7), 739-752. https://doi.org/10.1016/j.finel.2011.02.005

Goller, B., Beck, J.L. and Schueller, G.I. (2012), "Evidence-based identification of weighting factors in Bayesian model updating using modal data", *J. Eng. Mech.*, **138**(5), 430-440. https://doi.org/10.1061/(ASCE)EM.1943-7889.0000351

Govers, Y. and Link, M. (2010), "Stochastic model updating—covariance matrix adjustment from uncertain experimental modal data", *Mech. Syst. Signal Process.*, **24**(3), 696-706. https://doi.org/10.1016/j.ymssp.2009.10.006

Hastings, W. (1970), "Monte Carlo sampling methods using Markov chains and their applications", *Biometrika*, **57**(1), 97-109. https://doi.org/10.1093/biomet/57.1.97

Hirooka, T., Kim, C.W., Hayashi, G. and Goi, Y. (2021). "Vibration monitoring of a real steel plate girder bridge under artificial local damage and varying temperature", *EASEC16*, Brisbane, Australia.

Jaishi, B. and Ren, W.X. (2005), "Structural finite element model updating using ambient vibration test results", *J. Struct. Eng*, **131**(4), 617-628. https://doi.org/10.1061/(ASCE)0733-9445(2005)131:4(617)

Jaishi, B. and Ren, W.X. (2006), "Damage detection by finite element model updating using modal flexibility residual", *J. Sound Vib.*, **290**(1-2), 369-387. https://doi.org/10.1016/j.jsv.2005.04.006

Jang, J. and Smyth, A. (2017), "Bayesian model updating of a full-scale finite element model with sensitivity-based clustering", *Struct. Control Health Monitor.*, **24**(11), e2004. https://doi.org/10.1002/stc.2004

Katafygiotis, L.S. and Beck, J.L. (1998), "Updating models and their uncertainties. ii: model identifiability", *J. Eng. Mech.*, **124**(4), 463-467. https://doi.org/10.1061/(ASCE)0733-9399(1998)124:4(463)

Lam, H.F., Yang, J.H. and Au, S.K. (2015), "Bayesian model updating of a coupled-slab system using field test data utilizing an enhanced Markov chain Monte Carlo simulation algorithm", *Eng. Struct.*, **102**, 144-155. https://doi.org/10.1016/j.engstruct.2015.08.005

Lam, H.F., Yang, J.H. and Au, S.K. (2018), "Markov chain Monte Carlo-based Bayesian method for structural model updating and damage detection", *Struct. Control Health Monitor.*, **25**(4), e2140. https://doi.org/10.1002/stc.2140

Liu, P., Huang, S., Song, M. and Yang, W. (2021), "Bayesian model updating of a twin-tower masonry structure through subset simulation optimization using ambient vibration data", *J. Civil Struct. Health Monitor.*, **11**, 129-148. https://doi.org/10.1007/s13349-020-00443-y

Lye, A., Cicirello, A. and Patelli, E. (2021), "Sampling methods for solving Bayesian model updating problems: A tutorial", *Mech. Syst. Signal Process.*, **159**, 107760. https://doi.org/10.1016/j.ymssp.2021.107760

Mares, C., Mottershead, J.E. and Friswell, M.I. (2006), "Stochastic model updating: part 1—theory and simulated example", *Mech. Syst. Signal Process.*, **20**(7), 1674-1695. https://doi.org/10.1016/j.ymssp.2005.06.006

Metropolis, N., Rosenbluth, A.W., Rosenbluth, M.N. and Teller, A.H. (1953), "Equation of state calculations by fast computing machines", *J. Chem. Phys.*, **21**(6), 1087-1092. https://doi.org/10.1063/1.1699114

Mosegaard, K. and Tarantola, A. (1995), "Monte Carlo sampling of solutions to inverse problems", *J. Geophys. Res.*: *Solid Earth*, **100**(B7), 12431-12447. https://doi.org/10.1029/94JB03097

Mottershead, J.E. and Friswell, M.I. (1993), "Model updating in structural dynamics: a survey", *J. Sound Vib.*, **167**(2), 347-375. https://doi.org/10.1006/jsvi.1993.1340

Mottershead, J.E., Mares, C., James, S. and Friswell, M.I. (2006), "Stochastic model updating: part 2—application to a set of physical structures", *Mech. Syst. Signal Process.*, **20**(8), 2171-2185. https://doi.org/10.1016/j.ymssp.2005.06.007

Mottershead, J.E., Link, M. and Friswell, M.I. (2011), "The sensitivity method in finite element model updating: a tutorial", *Mech. Syst. Signal Process.*, **25**(7), 2275-2296. https://doi.org/10.1016/j.ymssp.2010.10.012

Muto, M. and Beck, J.L. (2008), "Bayesian updating and model class selection for hysteretic structural models using stochastic simulation", *J. Vib. Control*, **14**(1-2), 7-34. https://doi.org/10.1177/1077546307079400

Ni, Y.C. and Zhang, F.L. (2021), "Uncertainty quantification in fast Bayesian modal identification using forced vibration data considering the ambient effect", *Mech. Syst. Signal Process.*, **148**, 107078. https://doi.org/10.1016/j.ymssp.2020.107078

Ni, Y.C., Zhang, Q.W. and Liu, J.F. (2022), "Dynamic performance investigation of a long-span suspension bridge using a Bayesian approach", *Mech. Syst. Signal Process.*, **168**, 108700. https://doi.org/10.1016/j.ymssp.2021.108700

Pandey, A.K. and Biswas, M. (1994), "Damage detection in structures using changes in flexibility", *J. Sound Vib.*, **169**(1), 3-17. https://doi.org/10.1006/jsvi.1994.1002

Parzen, E. (1962), "On estimation of a probability density function and mode", *Annals Mathe. Statist.*, **33**(3), 1065-1076.

Ramancha, M.K., Astroza, R., Conte, J.P., Restrepo, J.I. and Todd, M.D. (2020), "Bayesian nonlinear finite element model updating of a full-scale bridge-column using sequential Monte Carlo", In: *Model Validation and Uncertainty Quantification*, Volume 3, Springer, Cham.

Ramancha, M.K., Astroza, R., Madarshahian, R. and Conte, J.P. (2022), "Bayesian updating and identifiability assessment of nonlinear finite element models", *Mech. Syst. Signal Process.*, **167**, 108517. https://doi.org/10.1016/j. ymssp.2021.108517

Patelli, E., Govers, Y., Broggi, M., Gomes, H.M., Link, M., and Mottershead, J.E. (2017), "Sensitivity or Bayesian model updating: a comparison of techniques using the DLR AIRMOD test data", *Arch. Appl. Mech.*, **87**(5), 905-925. https://doi.org/ 10.1007/s00419-017-1233-1

Rosenblatt, M. (1956), "Remarks on some nonparametric estimates of a density function", *Annals Mathe. Statist.*, **27**(3), 832-837.

Sehgal, S. and Kumar, H. (2016), "Structural dynamic model updating techniques: a state of the art review", *Arch. Computat. Methods Eng.*, **23**, 515-533. https://doi.org/10.1007/ s11831-015-9150-3

Simoen, E., De Roeck, G. and Lombaert, G. (2015), "Dealing with uncertainty in model updating for damage assessment: a review", *Mech. Syst. Signal Process.*, **56-57**, 123-149. https://doi.org/10.1016/j.ymssp.2014.11.001

Song, M., Yousefianmoghadam, S., Mohammadi, M.E., Moaveni, B., Stavridis, A. and Wood, R.L. (2018), "An application of finite element model updating for damage assessment of a two-story reinforced concrete building and comparison with lidar" *Struct. Health Monitor.*, **17**(5), 1129-1150. https://doi.org/10.1177/1475921717737970

Tierney, L. (1994), "Markov chains for exploring posterior distributions", *Annals Statist.*, **22**(4), 1701-1728.

Tran-Ngoc, H., He, L., Reynders, E., Khatir, S., Le-Xuan, T., De Roeck, G., Bui-Tien, T. and Wahab, M.A. (2020), "An efficient approach to model updating for a multispan railway bridge using orthogonal diagonalization combined with improved particle swarm optimization", *J. Sound Vib.*, **476**, 115315. https://doi.org/10.1016/j.jsv.2020.115315

Van Overschee, P. and De Moor, B.L. (2012), *Subspace identification for linear systems*: *Theory-Implementation-Applications*, Springer Science & Business Media.

Vanik, M.W., Beck, J.L. and Au, S.K. (2000), "Bayesian probabilistic approach to structural health monitoring", *J. Eng. Mech.*, **126**(7), 738-745. https://doi.org/10.1061/(ASCE)0733-9399(2000)126:7(738)

Worden, K., Farrar, C.R., Manson, G. and Park, G. (2007), "The fundamental axioms of structural health monitoring", *Proceedings of the Royal Society A*: *Mathematical*, *Physical and Engineering Sciences*, **463**(2082), 1639-1664. https://doi.org/10.1098/rspa.2007.1834

Xin, Y., Hao, H., Li, J., Wang, Z.C., Wan, H.P. and Ren, W.X. (2019), "Bayesian based nonlinear model updating using instantaneous characteristics of structural dynamic responses", *Eng. Struct.*, **183**, 459-474. https://doi.org/10.1016/j.engstruct.2019.01.043

Yin, S., Ding, S.X., Haghani, A., Hao, H. and Zhang, P. (2012), "A comparison study of basic data-driven fault diagnosis and process monitoring methods on the benchmark Tennessee Eastman process", *J. Process Control*, **22**(9), 1567-1581. https://doi.org/10.1016/j.jprocont.2012.06.009

Yuen, K.V. (2010), *Bayesian methods for structural dynamics and civil engineering*, John Wiley & Sons.

Zhang, F.L., Au, S.K. and Ni, Y.C. (2021), "Two-stage Bayesian system identification using Gaussian discrepancy model", *Struct. Health Monitor.*, **20**(2), 580-595. https://doi.org/10.1177/1475921720933523

Zhou, X., Kim, C.W., Zhang, F.L. and Chang, K.C. (2022), "Vibration-based Bayesian model updating of an actual steel truss bridge subjected to incremental damage", *Eng. Struct.*, **260**, 114226. https://doi.org/10.1016/j.engstruct.2022.114226

HJ